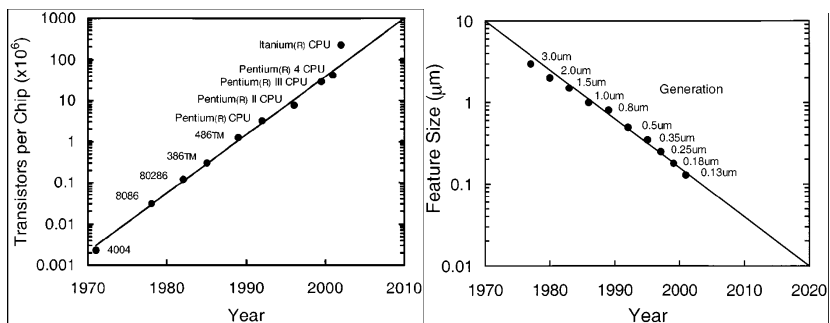


Transmission electron microscopy of semiconducting structures

T.Walther

Motivation for electron microscopy

- steady decrease in the size of many semiconductor devices, with a corresponding improvement in device performance and reduction in production costs. Moore's Law from 1965 stated that the number of transistor on a computer chip would double every 18-24 months.



MT Bohr, IEEE Trans. Nanotechnol. 1 (2002) 56-62



Motivation for electron microscopy

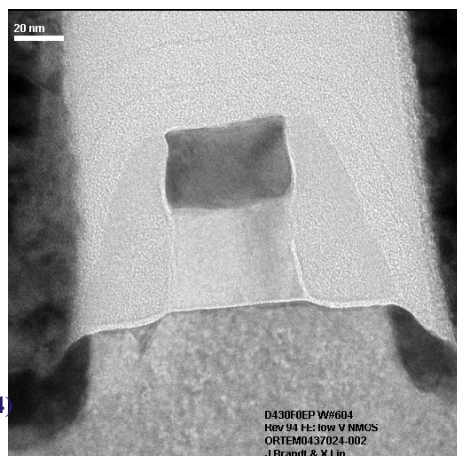
- continuing miniaturization only possible through detailed correlation of device properties with microstructure and chemistry on the nano-scale
- **electron microscopy** provides important research tools in the development and characterisation of new semiconductor device structures
- complements bulk analysis techniques such as X-ray diffraction or secondary ion mass spectroscopy and surface analytical techniques such as atomic force microscopy or scanning tunnelling microscopy.
- **transmission electron microscopy** and its associated analytical techniques provide the only real direct method of examining the internal structure of many of these devices at an **atomistic level**.



Motivation for electron microscopy

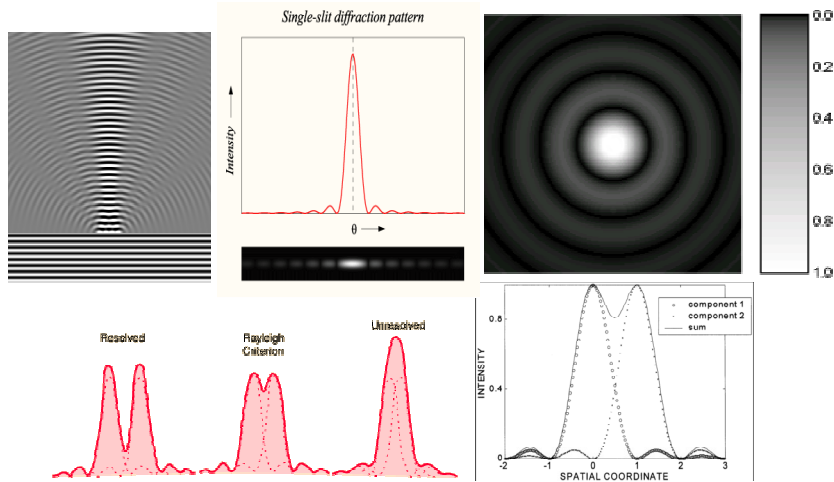
**lattice image of
currently smallest
CMOS transistor
with 35nm gate
length**

P. Bai et al., Proc. 50th IEEE
Intern. Electron Devices
Meeting, San Francisco (2004)
657-660



Comparison of electron with light microscopy

resolution improvement compared to light microscopy



Comparison of electron with light microscopy

resolution improvement compared to light microscopy

- resolution – defined as the smallest spacing of two points that can be observed as two distinct entities
- For a perfect lens system, resolution is limited by **diffraction**. The Rayleigh criterion states that the smallest spacing r between two resolved points is given by the distance at which the intensity maximum auf the central Airy disc falls into 1. minimum of the other [J. W. Strutt, (III. Lord Rayleigh), Philos. Mag. VIII (1879) 261, 403, 477]:

$$r = 0.61\lambda / (n \sin\alpha)$$

where λ = wavelength of illumination

n = refractive index

α = half angle subtended by an aperture

- blue light $\lambda = 400\text{nm}$, angle $\alpha=65^\circ$, oil with $n=1.56$: $r=194\text{nm} \approx 0.2\mu\text{m}$
- on-line simulation:
<http://www.olympusfluoview.com/java/resolution3d/index.html>



Comparison of electron with light microscopy

wavelength of fast electrons is much shorter than that of light

- electrons on the other hand, have wavelengths (that are useful for microscopy) of 1-10 millionth of that of visible light
- wavelength of electrons is related to their energy, i.e. accelerating voltage:
allowing for relativistic effects

$$\lambda^2 = h^2 / (2m_0eV + e^2V^2/c^2)$$

where: $c = 2.998 \times 10^8 \text{ m s}^{-1}$ velocity of light
 $e = 1.602 \times 10^{-19} \text{ C}$ charge on electron
 $h = 6.62 \times 10^{-34} \text{ Js}$ Planks Constant
 $m_0 = 9.109 \times 10^{-31} \text{ kg}$ rest mass of electron

This can be rearranged to give:

$$\lambda = [1.5/(V + 10^6 V^2)]^{1/2} \text{ nm}$$

for example: at 20kV: $\lambda = 0.0086 \text{ nm}$, 200kV: $\lambda = 0.0025 \text{ nm}$, 1000kV:
 $\lambda = 0.0009 \text{ nm}$



Comparison of electron with light microscopy

diffraction limit in electron microscopy

- for electrons in vacuum ($n=1$) and for small angles $\sin\alpha \approx \alpha$:

$$r = 0.61\lambda/\alpha$$

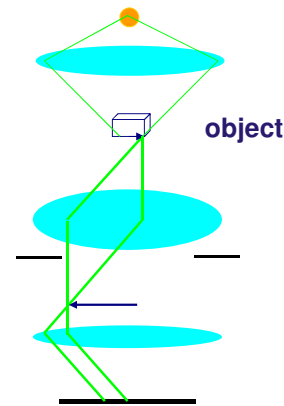
For a 200kV electron microscope where $\lambda = 0.00251 \text{ nm}$ with α typically 0.001-0.02 radians the diffraction limited resolution becomes 0.015-0.08nm for large and small apertures, respectively. This allows atomic resolution at 200kV in a transmission electron microscope (TEM)!

- actual resolution of a TEM instrument is not limited by wavelength but lens aberrations, which restrict the angular range that can be used (cf. Lecture 2).

Basics of emitters and electron optics

general optical elements necessary for a microscope

element	light
illumination source	light bulb
condenser	glass lens
objective	strong glass lens
aperture	pin-hole
projector	glass eye-piece
detector	eye, film, CCD



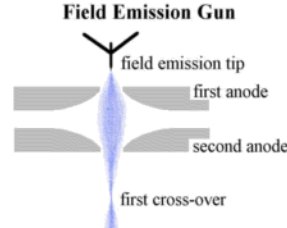
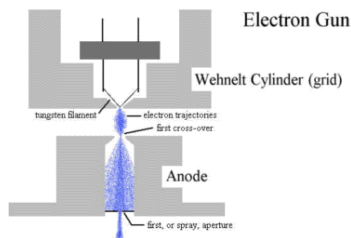
Basics of emitters and electron optics

general optical elements necessary for a microscope

element	light	electrons
illumination source	light bulb	cathode
condenser	glass lens	electromagnetic lens
objective	strong glass lens	electromagnetic lens
aperture	pin-hole	fine aperture
projector	glass eye-piece	electromagnetic lens
detector	eye, film, CCD	phosphor screen, film

Basics of emitters and electron optics

principles: heating to electron emission (thermal) or field-emission by strong electric field



cathodes principle	W filament thermal	LaB ₆ thermal	Schottky FEG thermal + field	cold FEG field-emission
virtual source size $2r$	~0.1mm	~μm	few nm	few Å
brightness $\beta = I(\pi r a)^2$ [$10^6 \text{ A/cm}^2 \text{sr}$]	~1	10-50	100-500	1000
vacuum [mbar]	10^{-5}	10^{-6}	10^{-9}	10^{-10}

Basics of emitters and electron optics

principle: use of Lorentz Force $F = -e(E + v \times B)$ to deflect electrons in an inhomogeneous field; result: no velocity change but rotation and focusing towards optical axis like a convex lens; problem: affects off-axis electrons stronger, hence spherical aberration

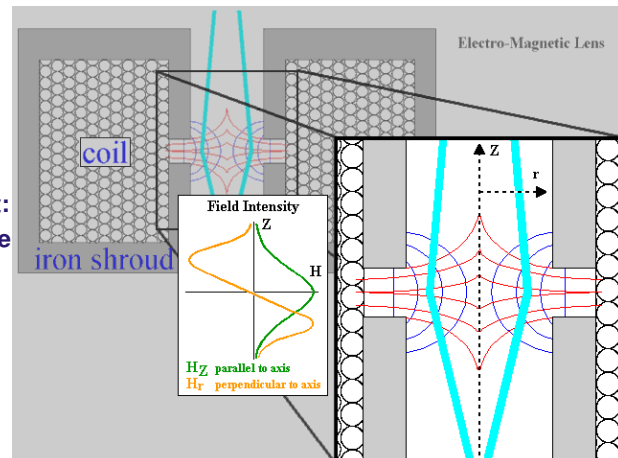


image courtesy by AR Sampson, Advanced Research Systems



Transmission electron microscopy (TEM) and Scanning transmission EM (STEM)

- used to study the internal structure and composition of materials
 - requires thin electron transparent specimens: <100nm thick
 - samples typically mounted on 3mm diameter disks or mesh grids
- specimens preparation a specialised procedure
 - typically material mechanically polished to 10-15 μ m thickness and reduced to electron transparency using Ar⁺ ion milling
 - non-conducting samples may require a thin coating with carbon to reduce charging
 - recent developments include the application of focused ion beam instruments to prepare site-specific cross-sections in lamella form



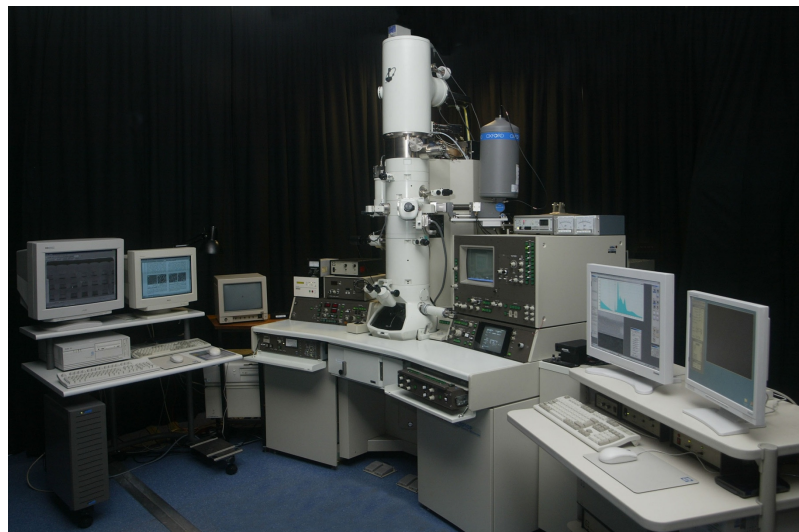
Structure of a TEM

- electron-optical column, with electromagnetic lenses, under high vacuum
- electrons generated in a **gun** and accelerated by application of a high voltage (typically 100kV – 1.25MV)
- electron spot formed on thin specimen using a 2- or 3-stage **condenser lens system** and aperture arrangement;
- 2 basic operation modes:
 - stationary convergent spot-mode illumination by condenser (de-magnifies electron source) or
 - transmission imaging operation with parallel beam illumination
- electrons transmitted by specimen pass through **objective lens**
 - magnified first **image formed in image plane**
 - **diffraction pattern simultaneously formed in back-focal plane**
- **intermediate and projector lenses** further magnify and project beam on to final fluorescent screen or photographic film/CCD camera for live recording
 - image magnifications from 50 up to 1.5x10⁶ directly displayed
 - TV camera/intensifier provides images up to >x10⁷ magnification
 - diffraction pattern can also be projected onto film/camera, depending on lens settings
- add-on detectors for chemical analysis and special signal recording



Structure of a STEM

- basic construction similar to that of TEM, but:
 - electron beam is focused and scanned in a raster across the specimen (as in an SEM but different from the static beam illumination used in a conventional TEM)
 - ultimate spatial resolution of a STEM depends on the probe forming capabilities of the illumination system: ~0.1nm now possible, i.e. atomic column chemical analysis by electron energy-loss spectroscopy (EELS)
 - needs ultra-high vacuum (UHV) to prevent sample contamination during long (serial) data acquisition
 - electrons transmitted through the sample are detected on a range of electron detectors
 - STEM imaging can be performed in either a dedicated instrument or a convention TEM equipped with a means to: form a small probe (need FEG source), scan the beam and record the image



Sheffield University JEOL 2010F TEM/STEM with add-on detectors



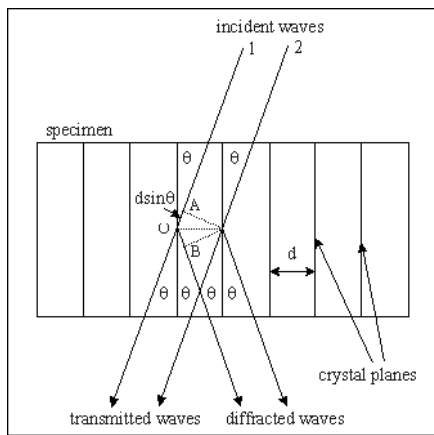
Signals and detectors

- for TEM imaging and diffraction:
 - phosphor screen, film (negative plates), TV camera, charge-coupled device (CCD) camera
- for BF and ADF-STEM imaging :
 - pneumatically retractable solid-state detectors
- for spectroscopy:
 - imaging energy filter for electron energy-loss spectrometer (EELS)
 - thin-window semiconductor detector for energy-dispersive X-ray spectroscopy (EDXS)
 - possibly other special detectors for secondary electrons, cathodoluminescence etc. (like in SEM);
problem: much weaker signals than in SEM (smaller volumes),
advantage: higher spatial resolution obtainable



Concept of electron diffraction

Bragg's Law



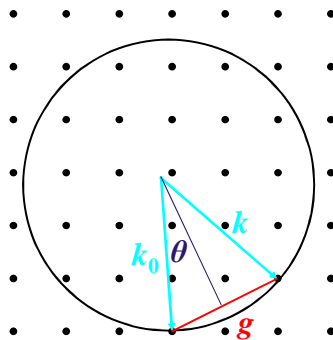
- optical path difference between diffracted waves 1 and 2 is $2d \sin \theta$
- If $2d \sin \theta = n\lambda$ then the waves are in-phase and interference with each other constructively
- therefore the conditions for diffraction :

$$2d \sin \theta = n\lambda$$

BRAGG'S LAW

Concept of electron diffraction

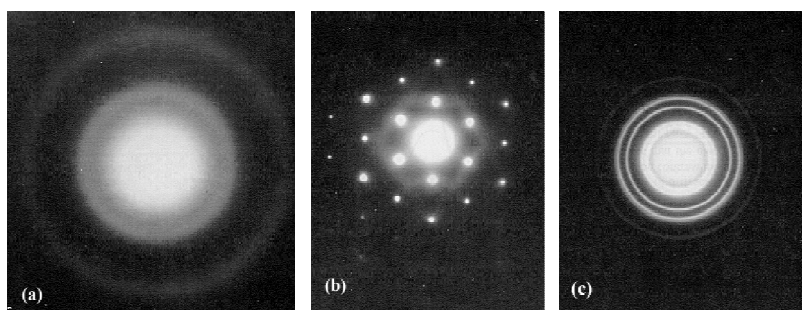
Ewald's sphere construction



construct so-called ‘reciprocal lattice’ with points of all crystal reflections, then draw circle with radius $k_0=1/\lambda$ and determine the directions for the incoming beam k_0 and the scattered beam k . Diffraction then occurs only if difference is a reciprocal lattice point, i.e.:
 $\sin \theta=n(g/2)/k_0=n\lambda/2d$
same result as Bragg’s Law!

Electron diffraction techniques

Selected-area electron diffraction (SAED) in the TEM



selected-area electron diffraction patterns obtained from three different materials: (a) amorphous carbon film, (b) Aluminium single crystal and (c) poly-crystalline gold; images courtesy of IM Ross, Univ. Sheffield



kinematical theory of diffraction contrast: the two-beam case

2-beam case:

- consider scattering of transmitted beam into **just one diffracted beam**
- consider parallel electron wave Ψ_0
- crystal consists of tiny unit cells of unity area, volume V_u and infinitely small thickness, dz , along beam direction; with structure factor $F(\theta)$
- > # of unit cells per unit area and thickness dz then is: dz/V_u
- each unit cell scatters into angle $\delta=2\theta$
- *change of scattered wave amplitude:*

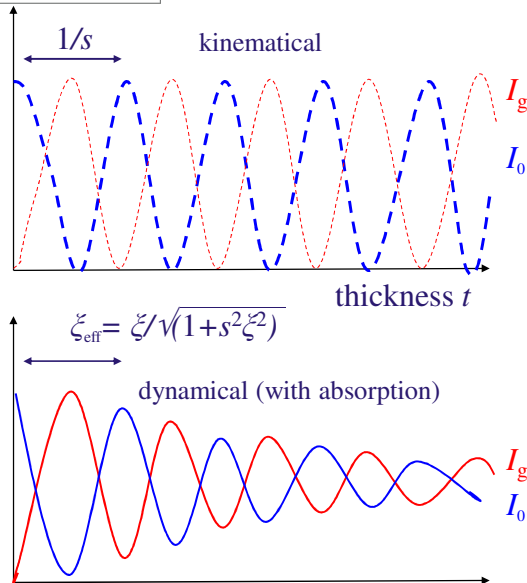
$$d\Psi_g = \Psi_0 / \cos(\theta) dz / V_u \int F(\theta) \exp(2\pi i k r) / r 2\pi r dr$$

$$\approx i \pi \Psi_0 \lambda F(\theta) / (\pi V_u) \exp(2\pi i k R) dz$$
- > integrate over foil thickness from 0 to t , define **extinction length** $\zeta = \pi V_u / [\lambda F(\theta)]$, use $R=t-z$ and **excitation error** $s = \mathbf{k} - \mathbf{k}_0 - \mathbf{g}$ and obtain

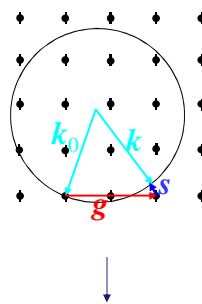
$$\Psi_g = i\pi / \zeta \exp(2\pi i k_0 t) \int_0^t \exp(-2\pi s z) dz$$
- **intensity** then is modulus square of this:
 $I_g = \Psi_g \Psi_g^* = \pi^2 / \zeta^2 \sin^2(\pi s) / (\pi s)^2$
- *therefore get intensity fluctuations as a function of depth in the foil!*
for $t =$ integer multiple of $1/s$ get $I_g = 0$



kinematical theory of diffraction contrast: the two-beam case



Ewald's sphere for thin crystal and excitation error s



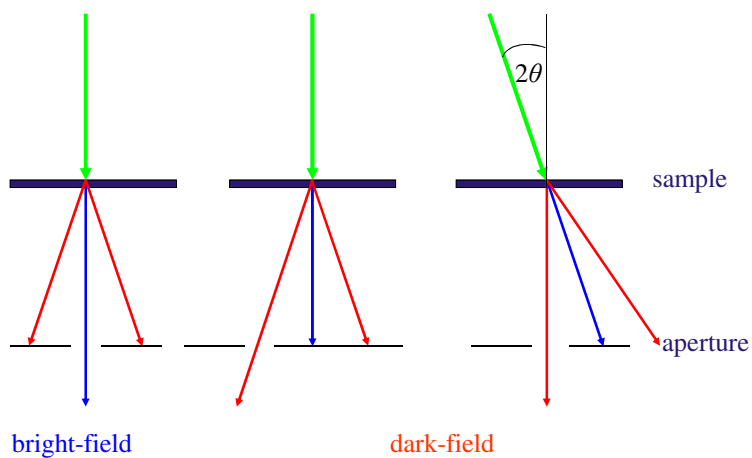
thickness fringes

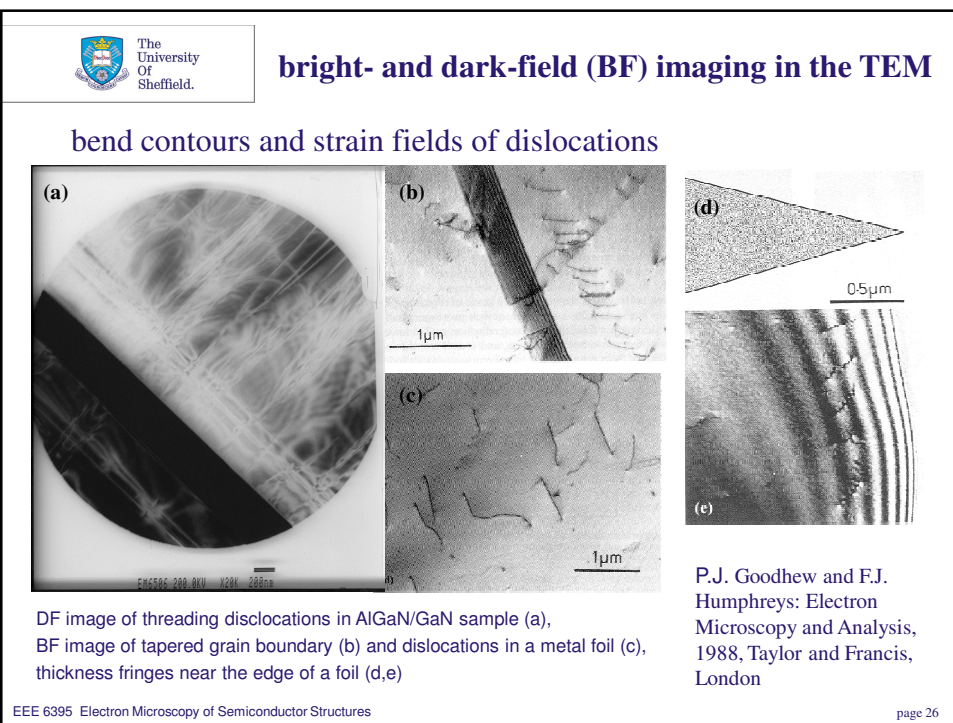
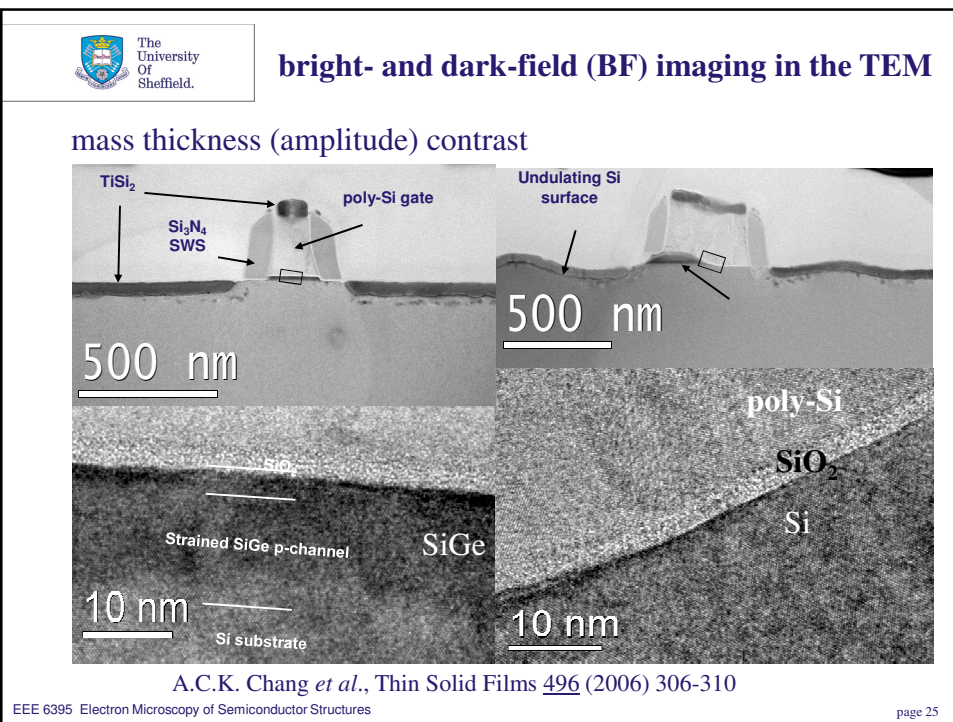
bright- and dark-field (BF) imaging in the TEM

mass thickness (amplitude) contrast

- scattered electrons have an altered energy spread and angular range relative to the primary beam
- inserting a small moveable **aperture** into the back-focal (diffraction) plane of the objective lens (objective aperture or high contrast aperture) selects the electrons allowed to form the final image:
 - aperture centred on the optical axis – regions of the specimen which are thicker or of higher density will scatter more strongly and appear darker in the final image – **bright-field image**
 - for crystalline samples, if particular diffracted beams are selected by aperture to contribute to the final image it is possible to obtain important information about crystal defects such as dislocations, stacking faults and precipitates – **dark-field image**

bright- and dark-field (BF) imaging in the TEM



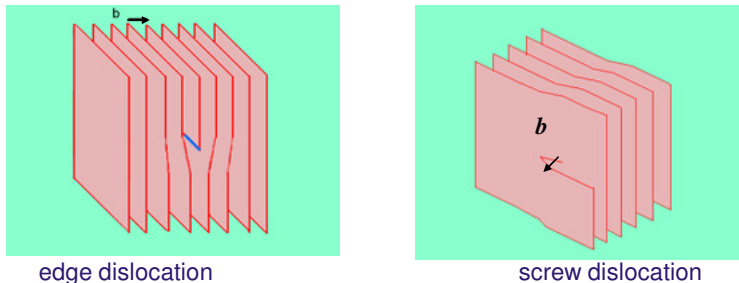


bright- and dark-field (BF) imaging in the TEM

bend contours and strain fields of dislocations

The strain field around a dislocation distorts the lattice. Only lattice planes with a component parallel to the Burgers vector \mathbf{b} are bent. If a diffraction vector \mathbf{g} is chosen so that \mathbf{g} and \mathbf{b} are perpendicular to each other, i.e. $\mathbf{g} \cdot \mathbf{b} = 0$, then the corresponding **strain field will be invisible!**

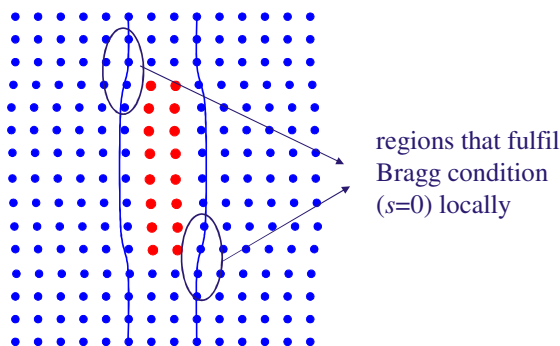
Note: conventional bright- and dark-field imaging visualises the strain field around a dislocation rather than the dislocation itself!



bright- and dark-field (BF) imaging in the TEM

strain contrast around inclusions and precipitates

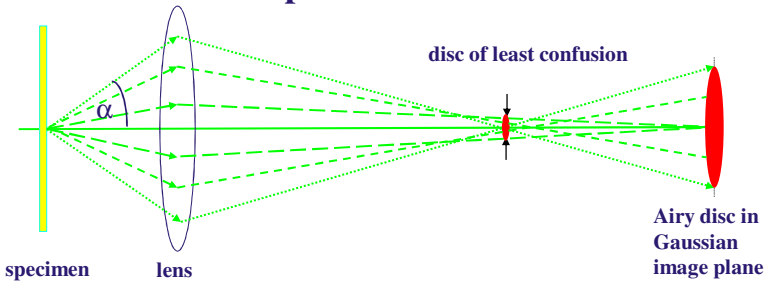
The strain field around a coherently strained precipitate can be imaged in the same way; the image contrast on either side of it provides information on both the sign of the strain (compressive or tensile) and its magnitude.



high-resolution electron microscopy (HREM)

lens aberrations

spherical aberration



The portion of the lens furthest from the optical axis brings rays to focus nearer the lens than the central portion of the lens. This results in a disc of least confusion of diameter d that is related to α (the semi-angle at which rays leave points on the specimen) by:

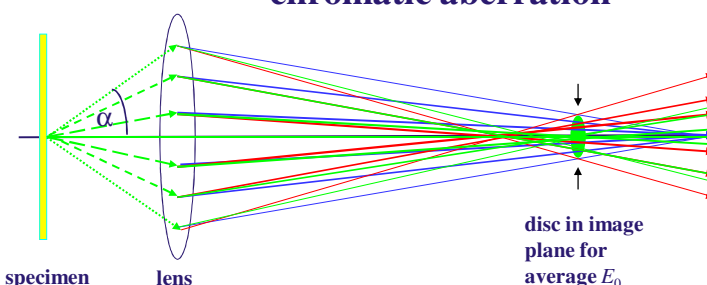
$$d_{\min} = 0.5 C_s \alpha^3$$

Note the corresponding Airy disc in the Gaussian image plane is 4 times as large!
 C_s is called spherical aberration constant; for most instruments it is ~ 1 mm.

high-resolution electron microscopy (HREM)

lens aberrations

chromatic aberration



Waves of different wavelength are present in both the primary beam and those emerging from a thin specimen – **chromatic aberration** describes the effect that slower electrons (red) are brought to focus by a lens nearer the lens than faster electrons (blue). This chromatic disc diameter in the Gaussian image plane is given by:

$$d_c = 0.5 C_c \alpha \Delta E / E_0 [1 + E_0/m_0 c^2] / [1 + E_0/2m_0 c^2]$$

where ΔE is the energy loss and E_0 is the energy of the primary beam and C_c the chromatic aberration constant.



high-resolution electron microscopy (HREM)

image formation: transfer theory and non-linear imaging

- phase contrast:
 - Relative **phase shifts** are introduced into the scattered electron waves by different regions of the sample.
 - When many beams are accepted by the objective aperture and interfere with the main (un-scattered) beam **constructive and destructive interference** occurs.
 - With correct defocus and at very high magnification, the image shows phase contrast which can reveal detail of the corresponding crystal lattice – **high resolution transmission electron microscopy** (HREM)
 - Can show atomic columns running through the crystal as dark or bright features – care required for interpretation; necessary to perform image simulation to confirm experimental data!



high-resolution electron microscopy (HREM)

image formation: transfer theory and non-linear imaging
transfer function

The objective lens induces a **phase shift** $\exp(-i\chi)$ of the electron beam where the **contrast transfer function** is in first order given by

$$\chi(g) = \pi/2(C_s \lambda^3 g^4 + 2f\lambda g^2)$$

where C_s is the spherical aberration coefficient, λ is the wavelength of the incident electrons, g the reciprocal lattice vector and f the defocus. This means both focus and spherical aberration determine the contrast of the atomic columns, and they act in the opposite direction.



high-resolution electron microscopy (HREM)

image formation: transfer theory and non-linear imaging imaging

Consider a wavefunction at the bottom of a specimen whose amplitude and phase have been a little modulated by interacting with the specimen:

$\Psi_s(r) = A \exp(i\varphi) \sim 1 - a(r) + i\varphi(r)$ where a denotes the decrease in amplitude compared to the incident wave (unity). Assume the specimen has only a single spatial frequency q along x :

$$\Psi_s(x) = 1 + [-a(x) + i\varphi(x)] \cos(2\pi q x)$$

This wave is now modulated by the contrast transfer function of the microscope:

$$\Psi_f(x) = 1 + [-a(x) + i\varphi(x)] \cos(2\pi q x) \exp(-i\chi)$$



high-resolution electron microscopy (HREM)

image formation: transfer theory and non-linear imaging imaging

The intensity then is the modulus square of this wave-function:

$$\begin{aligned} I(x) = & 1 + \frac{1}{2} (a^2 + \varphi^2) \\ & - 2a(x) \cos(2\pi q x) \cos\chi(q) \\ & + 2\varphi(x) \cos(2\pi q x) \sin\chi(q) \\ & + \frac{1}{2} (a^2 + \varphi^2) \cos(4\pi q x) \end{aligned}$$

This shows that the amplitude is transferred with $\cos\chi$ and the phase with $\sin\chi$. The **weak phase object (WPO) approximation** means $a \sim 0$ so that only the phase transfer needs to be considered. Also note the last term: an **artificial double frequency** (finer detail) has appeared!



high-resolution electron microscopy (HREM)

point resolution

If we take the effects of spherical aberration into consideration and combine this with the defocusing at the Scherzer focus for which the contrast transfer function shows a broad transfer and atomic columns appear dark we get the **point resolution**:

$$r_{\text{point}} \approx 0.66(C_s \lambda^3)^{1/4}$$

where C_s is the spherical aberration coefficient and λ is the wavelength of the incident electrons. Hence, for a 200kV TEM with a C_s of 0.5mm the point resolution is $r \approx 0.19\text{nm}$. Information can be transferred down to the **information limit** $0.43(C_s \lambda^3)^{1/4} \approx 0.13\text{nm}$, **but the details are not directly interpretable any more.**

NB: for aberration corrected HREM, $C_s \approx 0$ and instead of the above equation one needs to consider higher-order aberrations. For our new 300kV instrument with double aberration correction, $r_{\text{point}} \approx 0.05\text{nm}$.



high-resolution electron microscopy (HREM)

lattice fringe spacings

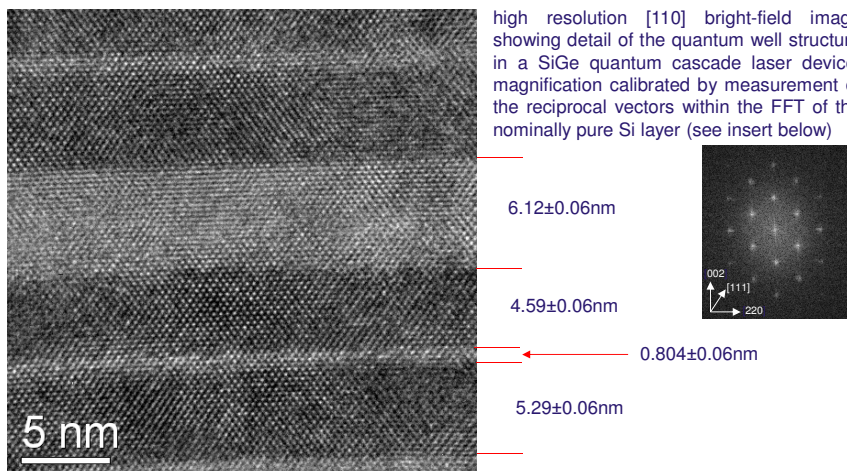


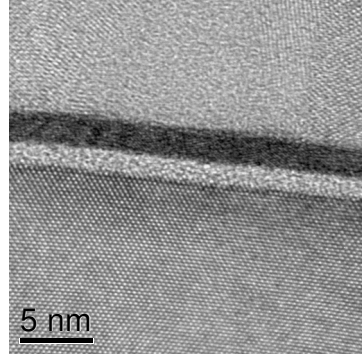
image courtesy of I.M. Ross, University of Sheffield

high-resolution electron microscopy (HREM)

lattice fringe spacings: more examples



high resolution TEM cross-section of an InAs/GaAs (001) quantum dot showing atomic columns

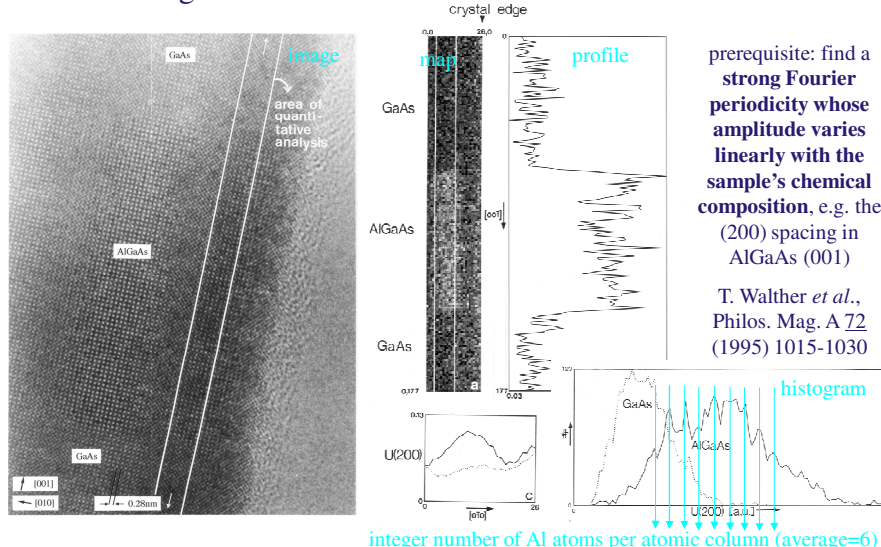


high resolution TEM cross-section of the gate oxide layer in a state-of-the-art transistor device

images courtesy of I.M. Ross, University of Sheffield

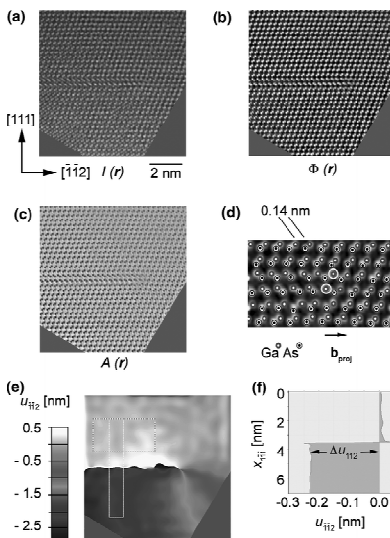
high-resolution electron microscopy (HREM)

lattice fringe contrast: chemical lattice imaging



high-resolution electron microscopy (HREM)

exit surface reconstruction



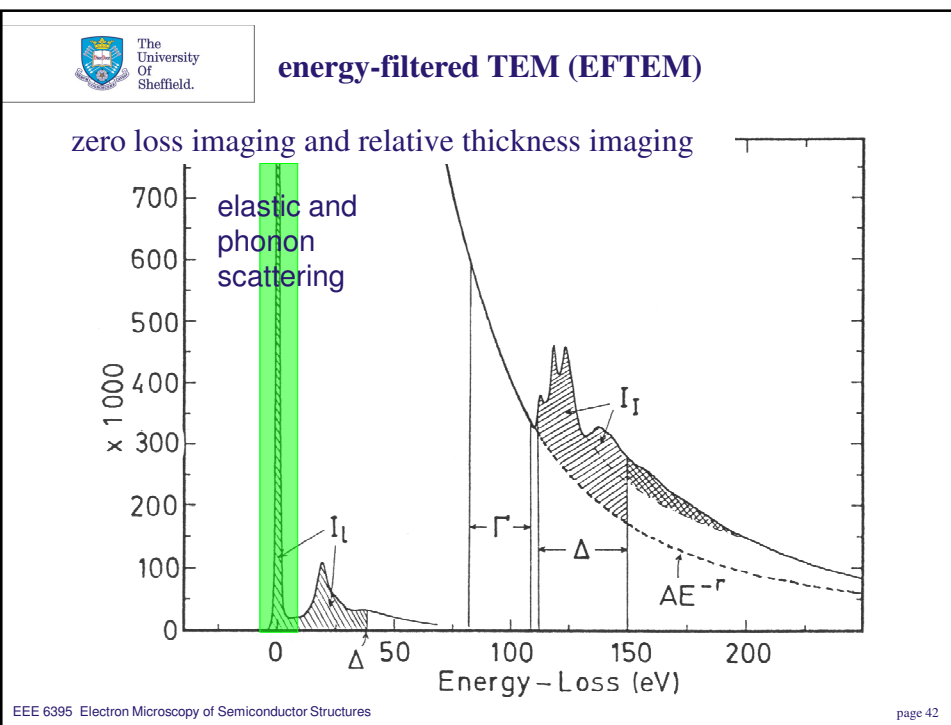
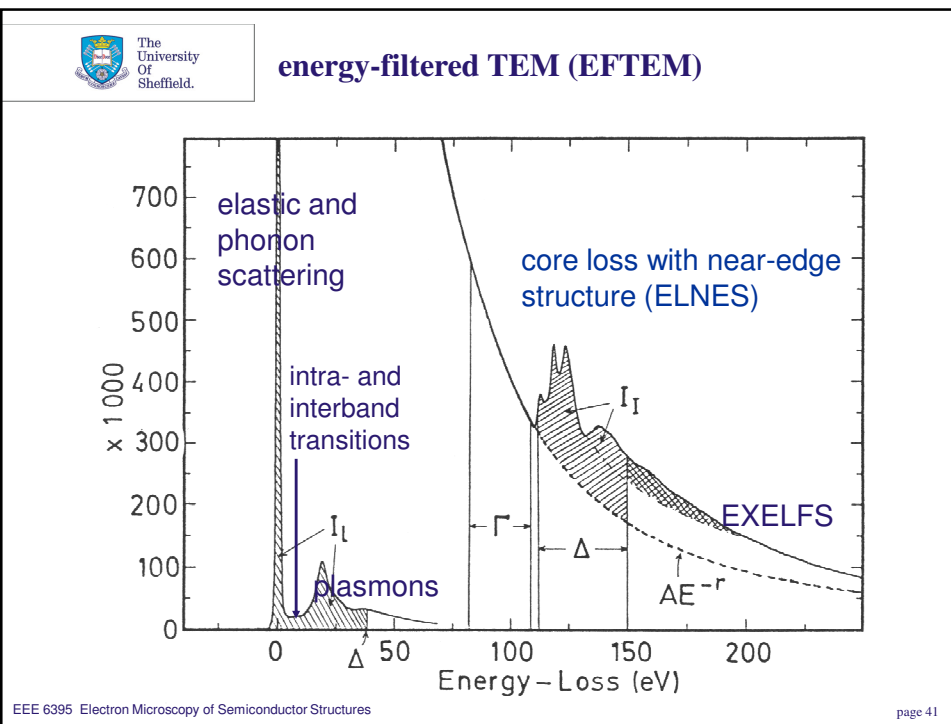
principle: get complex wave-function of the electron in amplitude A and phase Φ at bottom surface of specimen from:

- a) focus series,
 - b) beam tilt series or
 - c) holography
- + extensive computer calculations

K. Tillmann *et al.*, J. Mat. Sci. 41 (2006)
4420-4433

energy-filtered TEM (EFTEM)

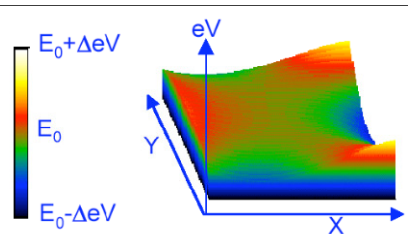
- principle:
use imaging energy filter and slit aperture to select scattered electrons of a certain energy window and use electron energy-loss spectrum to interpret the image contrast
- main applications of EFTEM:
 - **contrast enhancement**
to improve visibility – particularly useful in biological specimens
 - **elemental mapping**
to investigate the elemental distribution within a specimen
 - **chemical state mapping**
to reveal the chemical states within a sample by enhancing the contrast in the image as a function of chemical state



energy-filtered TEM (EFTEM)

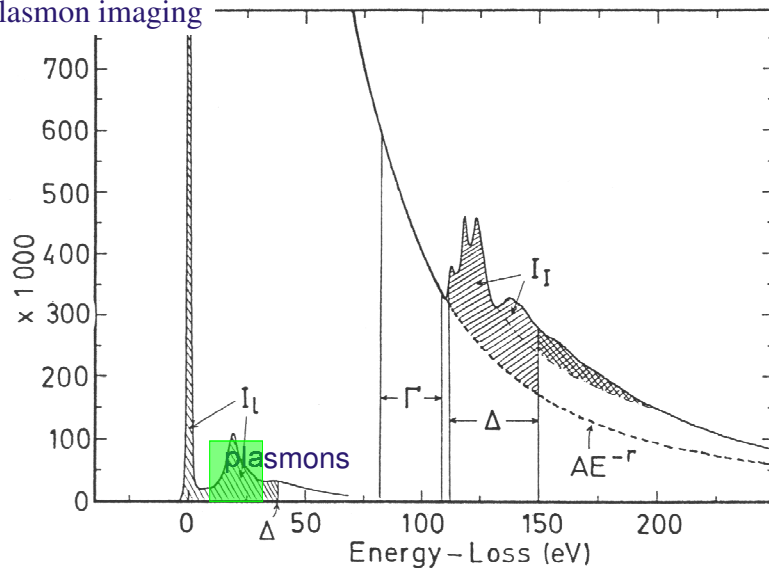
zero loss imaging and relative thickness imaging

- principle: use small slit aperture to select only elastically scattered electrons around the zero loss peak;
gives improved contrast (chromatic aberrations reduced);
 can be used to calculate relative thickness map from log of ratio of unfiltered to elastic intensity in terms of **inelastic mean free path L** :
 $t/L = \ln(I_{\text{total}}/I_0)$
- limit: non-isochromaticity of filter



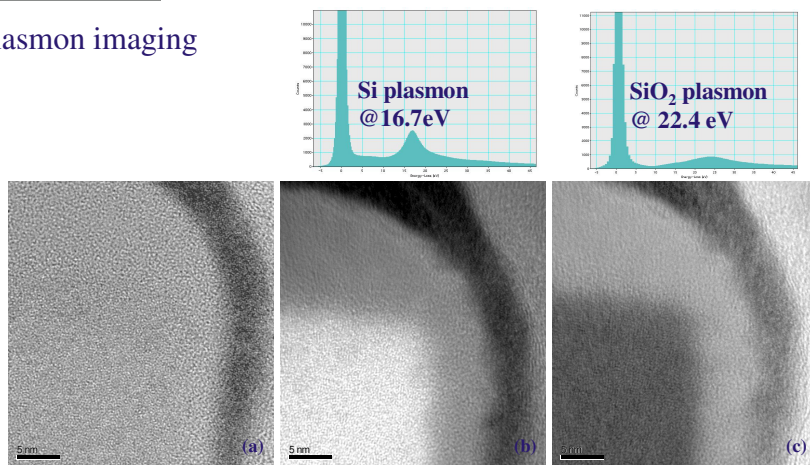
energy-filtered TEM (EFTEM)

plasmon imaging



energy-filtered TEM (EFTEM)

plasmon imaging

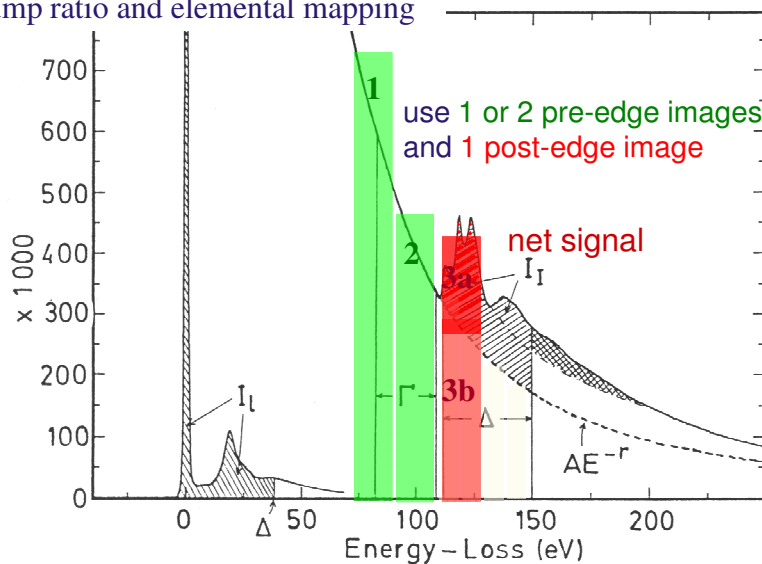


Higher magnification TEM images of the top right-hand corner of the device, (a) bright-field zero-loss image, (b) Si plasmon image and (c) SiO₂ plasmon image highlighting the distinction between the *amorphous* upper gate electrode region and the amorphous poly re-oxide layer.

data courtesy of I.M. Ross, University of Sheffield

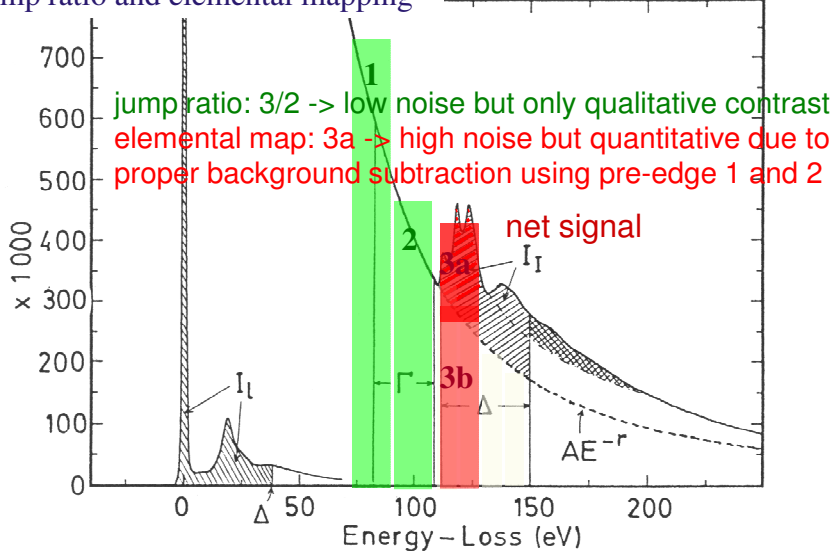
energy-filtered TEM (EFTEM)

jump ratio and elemental mapping



energy-filtered TEM (EFTEM)

jump ratio and elemental mapping

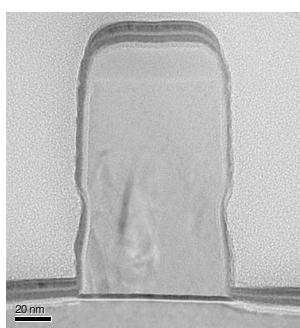


EEE 6395 Electron Microscopy of Semiconductor Structures

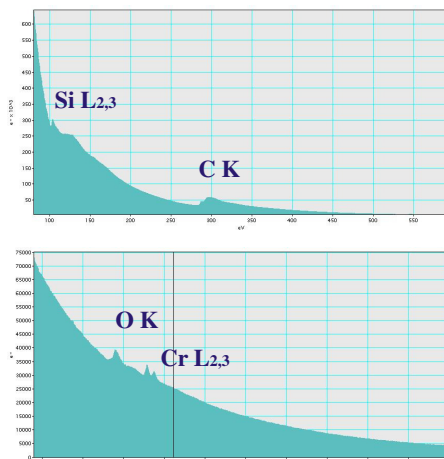
page 47

energy-filtered TEM (EFTEM)

jump ratio and elemental mapping



TEM bright-field and energy-filtered TEM (EFTEM) image of a transistor device. Right: corresponding EELS spectra derived from the whole device.



images courtesy of I.M. Ross, University of Sheffield

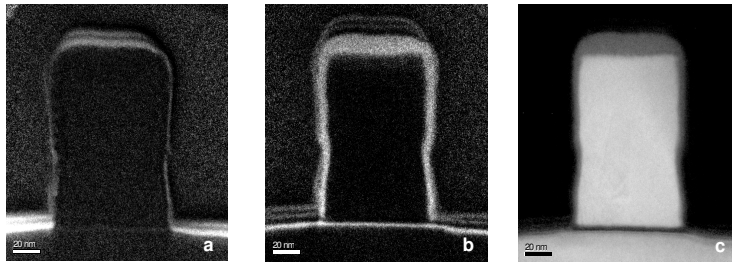
EEE 6395 Electron Microscopy of Semiconductor Structures

page 48



energy-filtered TEM (EFTEM)

jump ratio and elemental mapping



Single stack transistor device: Energy-filtered TEM (EFTEM) images showing (a) chromium, (b) oxygen and (c) silicon distributions respectively.

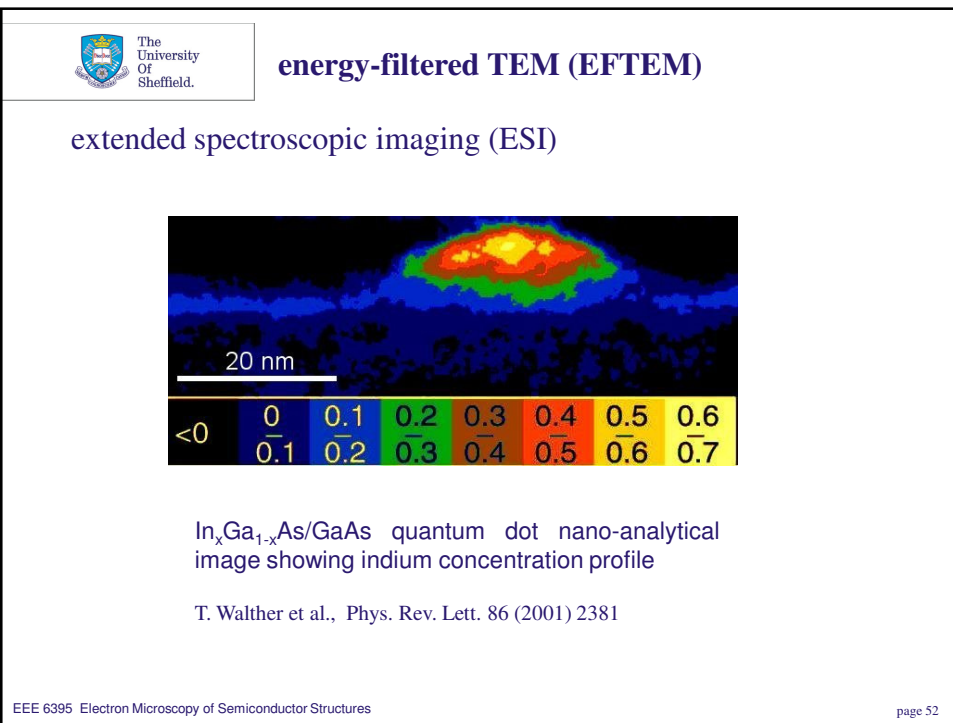
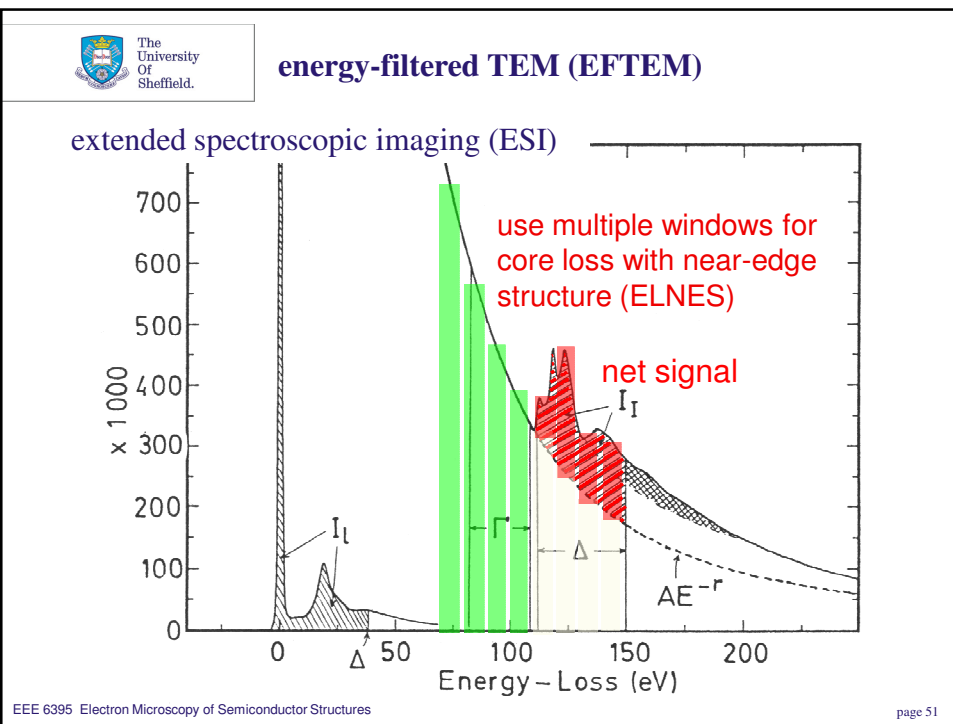
images courtesy of I.M. Ross, University of Sheffield



energy-filtered TEM (EFTEM)

jump ratio and elemental mapping

- spatial resolution of inner-shell loss images depends on several factors; ~1nm spatial resolution attainable in the best case:
 - **delocalisation of inelastic scattering** – ionisation of an atom by a fast electron which is some distance away
 - **diffraction limit due to objective aperture**
 - **spherical aberration of the objective lens (C_s)**
 - **chromatic aberration of the objective lens (C_c)**
 - **statistical noise due to low inelastic cross sections**
 - **radiation damage of the specimen**
 - **instrumental instabilities** – high voltage drift, sample drift, contamination etc



The University Of Sheffield.

scanning transmission EM (STEM)

D.B. Williams and C.B. Carter: TEM– Vol.1: Basics, Springer, New York, 1996, p. 146

EEE 6395 Electron Microscopy of Semiconductor Structures

page 53

The University Of Sheffield.

scanning transmission EM (STEM)

high-angle annular dark-field (HA-ADF) imaging or ‘Z-contrast’

- HAADF image** is formed by using a large annular detector. Regions of the specimen which scatter electrons through high angles (>50mrad) are recorded and appear with bright contrast in the final image.
- In the HAADF image the image intensity increases with specimen thickness and average number (Z) of the specimen. Regions of high Z appear with brighter contrast compared to regions of lower Z . Quantification is possible, because **for large angles Rutherford scattering dominates** the elastic scattering. A screened atomic nuclear potential of form $V(r)=Ze(4\pi\epsilon_0 r)^{-1}\exp(-r/r_0)$ with $r_0=(\theta_0 k_0)^{-1}$ yields the **differential scattering cross-section**, $\delta\sigma/\delta\Omega$, for $q=2k_0\sin(\theta/2)$:

$$\delta\sigma_e/\delta\Omega = 4\gamma^2 a_0^{-2} |Z-f_x(q)|^2 q^{-4} \text{ where } \gamma=(1-v^2/c^2)^{-1/2} \text{ and } a_0=0.053\text{nm}$$

$$\rightarrow 4\gamma^2 Z^2 a_0^{-2} k_0^{-4} [\theta^2 + \theta_0^2]^{-2}$$

E. Rutherford, Philos. Mag. 21 (1911) 669

- The contrast in HAADF is generally unaffected by small changes in objective defocus and specimen thickness.

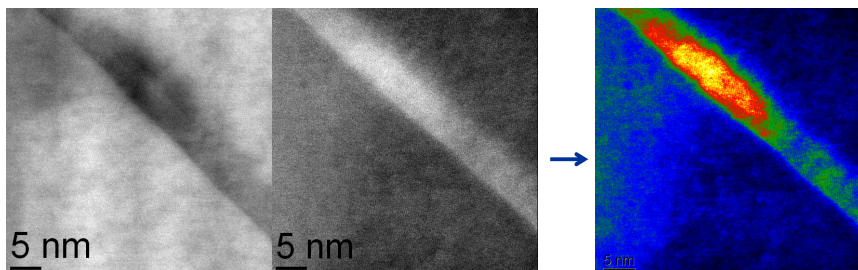
EEE 6395 Electron Microscopy of Semiconductor Structures

page 54



scanning transmission EM (STEM)

high-angle annular dark-field (HA-ADF) imaging or ‘Z-contrast’

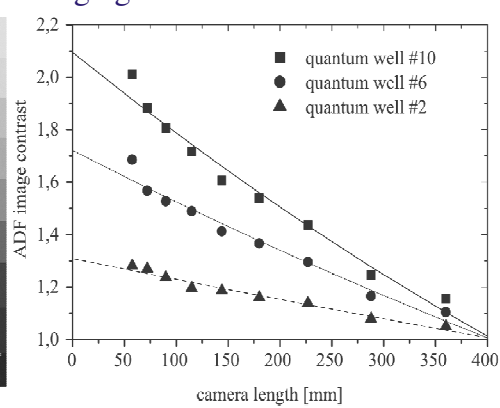
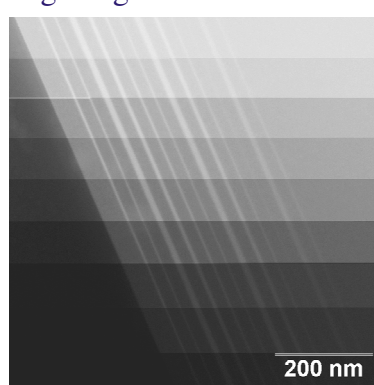


Bright-field (left) and annular dark-field (ADF, centre) lattice images of InAs quantum dots. Right: false-color map of indium concentration from square root of the high-angle ADF image intensity which, for a planar sample and after dark current correction, is a linear map of the chemical concentration x in the $\text{In}_x\text{Ga}_{1-x}\text{As}$ system.



scanning transmission EM (STEM)

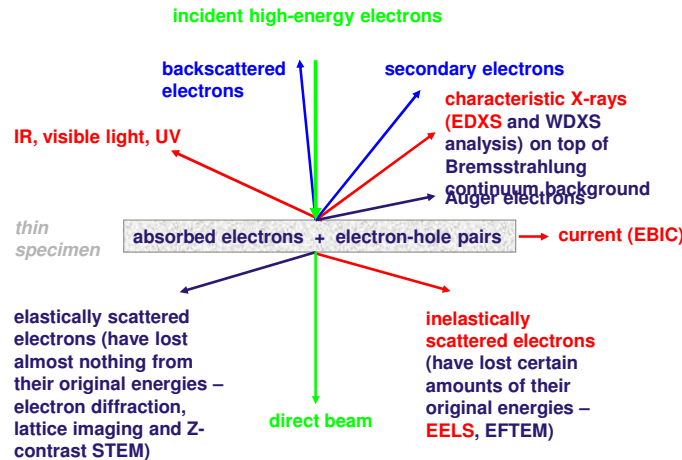
high-angle annular dark-field imaging or ‘Z-contrast’



parabolic extrapolation of the elastic image contrast vs. camera length to zero yields contrast for ideal Rutherford scattering at infinite scattering angle

T. Walther, J. Microsc. 221 (2006) 137-144

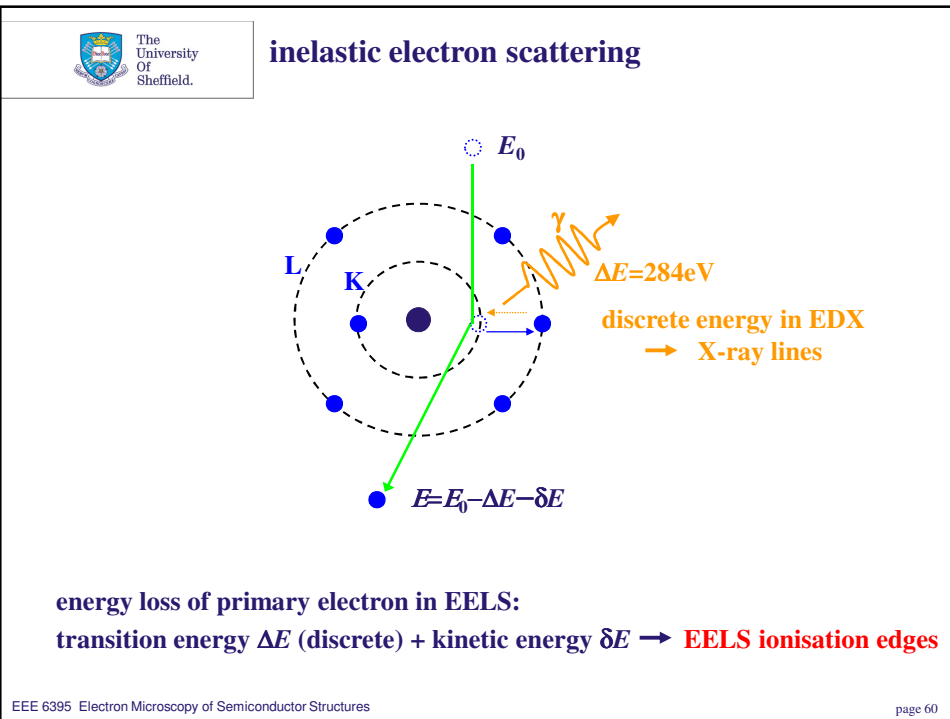
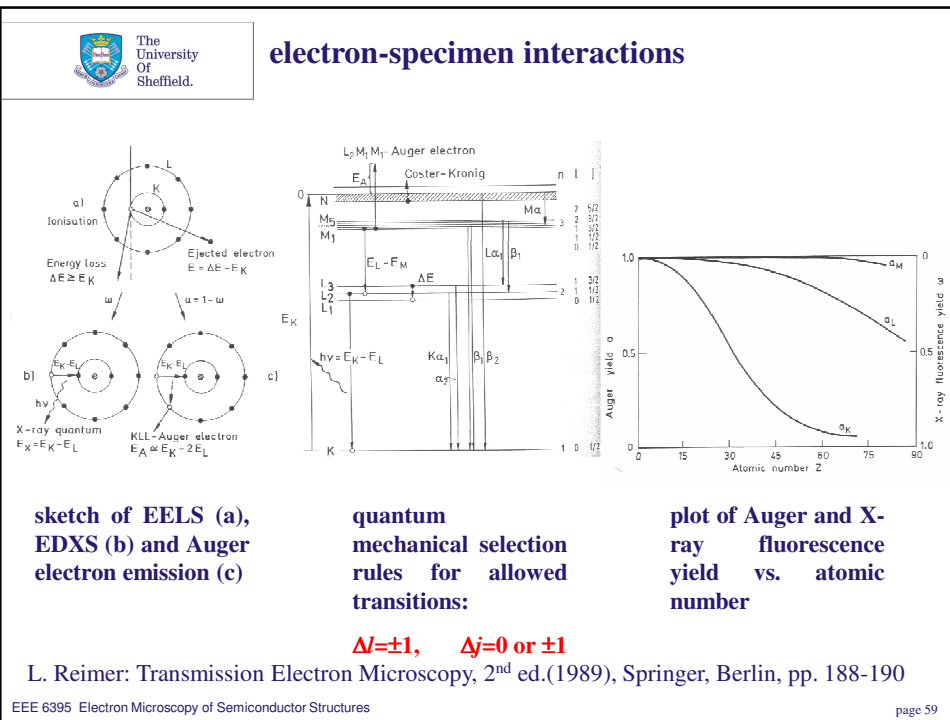
electron-specimen interactions

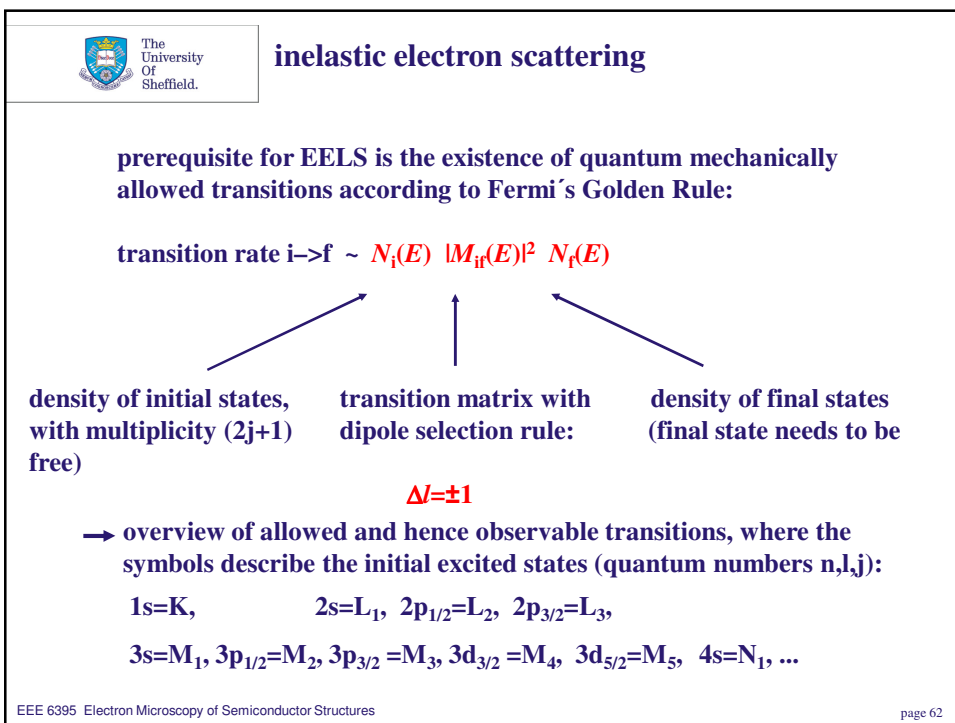
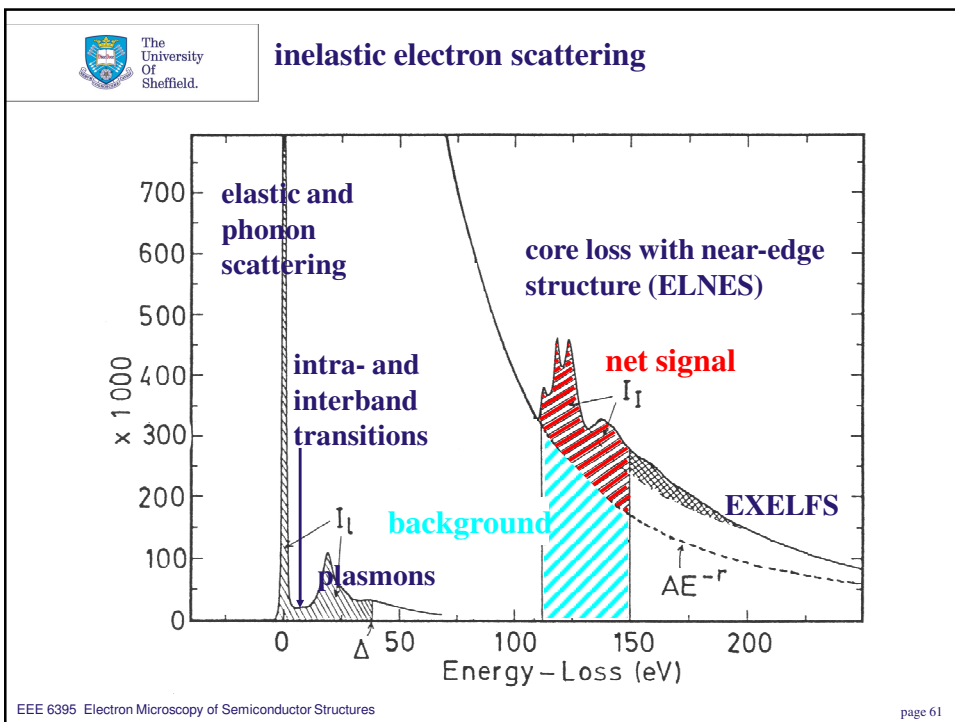


electron-specimen interactions

- first: ionisation of atom (excitation as primary effect)
 - The primary electron interacts with bound electrons. By exciting an electron from e.g. the innermost orbital (K-shell) it loses at least the ionisation energy, i.e. $\Delta E = E_K + \delta E \geq E_K$ and is (slightly) deflected -> EELS
- then: de-excitation (secondary effects)
 - radiative by emission of an X-ray of discrete energy, e.g. $E_\gamma = E_K - E_L$ with a probability given by X-ray fluorescence yield for transition from K to L-shell -> EDXS
 - or
 - non-radiative by transfer of energy to another (*third*) electron which is then ejected as an Auger electron of energy $E_A = E_K - E_L - E_I \approx E_K - 2E_L$, where E_I is the ionisation energy of this electron in the presence of a vacancy in a sub-shell, taking relaxation into account

-> Auger electron emission







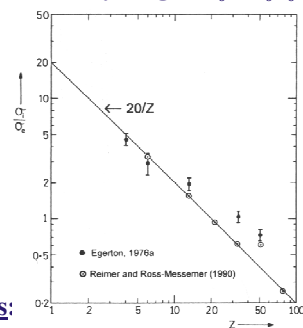
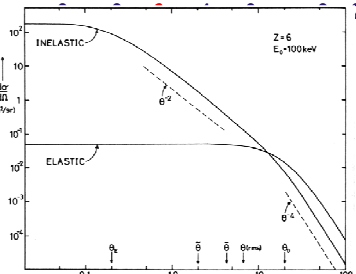
inelastic electron scattering

differential scattering cross-section, $\delta\sigma/\delta\Omega$, for scattering vector $q=2k_0\sin(\theta/2)$:
elastic, for scattering at the screened potential of the nucleus

(Rutherford):

$$\delta\sigma_e/\delta\Omega = 4\gamma^2 a_0^{-2} |Z - f_x(q)|^2 q^{-4}$$

for $V(r) = Ze (4\pi\epsilon_0 r)^{-1} \exp(-r/r_0)$
with decay length $r_0 = (\theta_0 k_0)^{-1}$



inelastic, for scattering by the bound electrons:

$$\delta\sigma_i/\delta\Omega = 4\gamma^2 a_0^{-2} Z q^{-4} \{1 - [1 + q^2 r_0^2]^{-2}\}$$

$$\rightarrow 4\gamma^2 a_0^{-2} Z k_0^{-4} [\theta^2 + \theta_E^2]^{-2} \{1 - [\theta_0^4 (\theta^2 + \theta_E^2 + \theta_0^2)^{-2}]\}$$

gives **Lorentzian function of narrow angular width** $\theta_E \approx 0.1\text{mrad}$
at average energy loss and steep decrease above $\theta_0 \approx 1\text{-}10\text{mrad}$



energy-dispersive X-ray spectroscopy (EDXS)

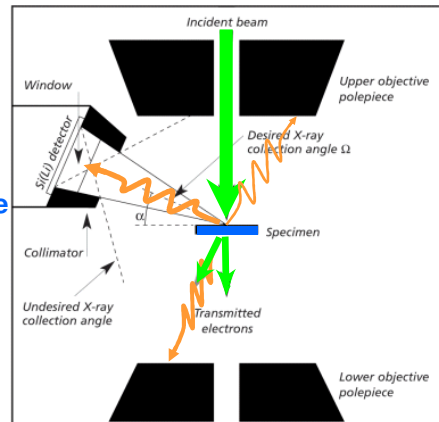
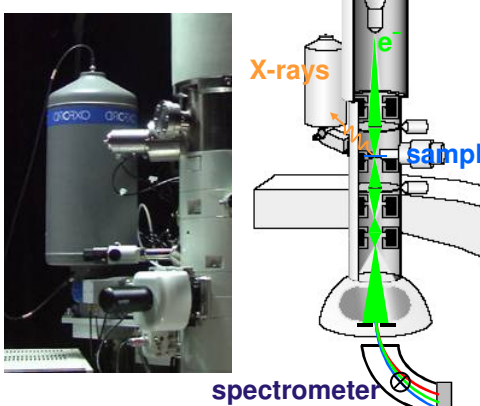
principles of X-ray generation and detection

- small fraction of X-Rays emitted isotropically by irradiated specimen are collected and analysed
 - X-ray detector provides a spectrum of photon intensity as a function of photon energy (hence the name energy-dispersive)
- Each element produces a series of characteristic X-rays on top of a weak background of Bremsstrahlung
 - EDXS can be used to detect the presence of specific elements within the specimen interaction volume (generally for elements above sodium).
 - *qualitative analysis*: provides information about which elements are present.
 - As the number of X-ray counts of a specific energy is in first approximation proportional to the amount of the element present it is possible to obtain *quantitative analysis* - information about the amount or relative amounts of each element present (after appropriate processing).
- single spot analysis or generate elemental distribution maps / profiles

energy-dispersive X-ray spectroscopy

principles of X-ray generation and detection

X-ray detector in (S)TEM



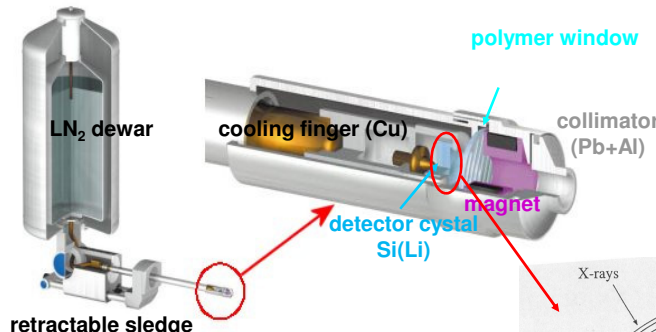
D.B. Williams and C.B. Carter: Transmission Electron Microscopy – IV: Spectrometry, Springer, New York, 1996

EEE 6395 Electron Microscopy of Semiconductor Structures

page 65

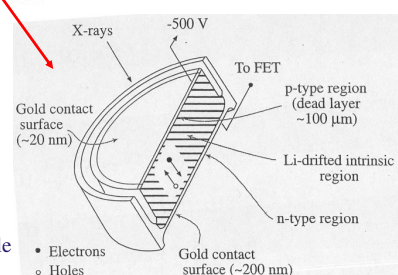
energy-dispersive X-ray spectroscopy

principles of X-ray generation and detection



- X-ray generates photo-electron
- photo-electron ionises atoms, generating electron-hole pairs
- # of electron-hole pairs is proportional to X-ray energy
- high voltage separates electron-hole pairs
- current is measured
- needs cooling to suppress thermal generation of electron-hole pairs and to prevent out-diffusion of Li in Si(Li) detector

EEE 6395 Electron Microscopy of Semiconductor Structures

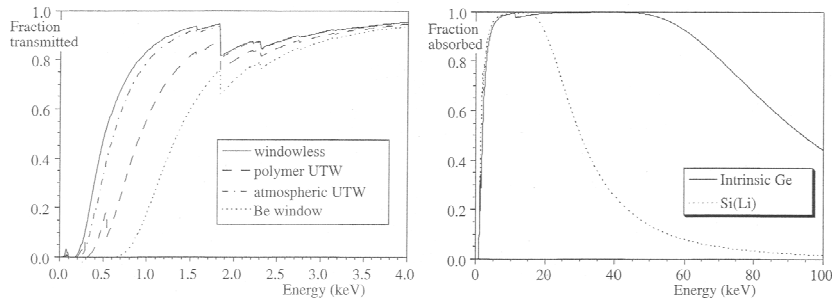


page 66



energy-dispersive X-ray spectroscopy

principles of X-ray generation and detection



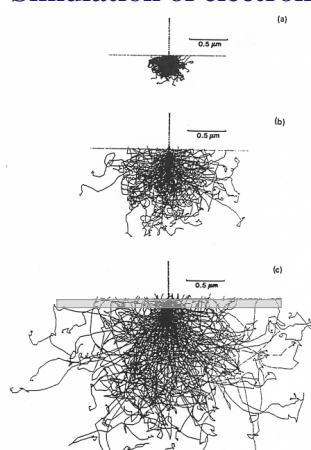
rôle of absorption by detector window material (left) and detector material itself (right) on sensitivity. In Si, it takes ~3.8eV, in high-purity Ge only ~2.9eV energy to generate an electron-hole pair.

D.B. Williams and C.B. Carter: Transmission Electron Microscopy – IV: Spectrometry, Springer, New York, 1996



energy-dispersive X-ray spectroscopy

Simulation of electron beam broadening



TEM vs. SEM: The spatial resolution of EDX analysis in the SEM is limited to ~1μm due to beam broadening within the interaction volume. In the TEM it can reach ~2nm because in a thin foil specimen the pear-shaped interaction volume is cut off.

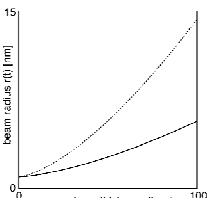
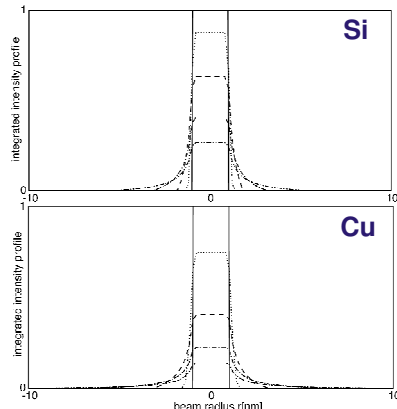
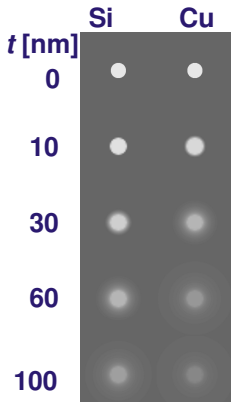
Random walk ('Monte Carlo') simulations of electron paths taking into account side-wards and inelastic scattering yield estimates of the beam broadening and the backscattered electron yield.

The broadening of the electron beam with sample thickness in TEM can also be calculated analytically to good approximation.

Monte Carlo calculations of the interaction volume in iron as a function of accelerating voltage: (a) 10kV, (b) 20kV (c) 30kV

energy-dispersive X-ray spectroscopy

Simulation of electron beam broadening



T. Walther,
J. Microsc. 215
(2004) 191

for 2nm \varnothing electron probe at 200kV, beam radius increase is:

$$\Delta r[\text{cm}] = 7 \times 10^5 Z / U (\rho/\text{A})^{0.5} t^{1.5}$$

J.I. Goldstein et al., Scanning Electron Microsc. 1 (1977) 315

energy-dispersive X-ray spectroscopy

spectrum analysis procedures

3 major effects are to be taken into account for quantification:

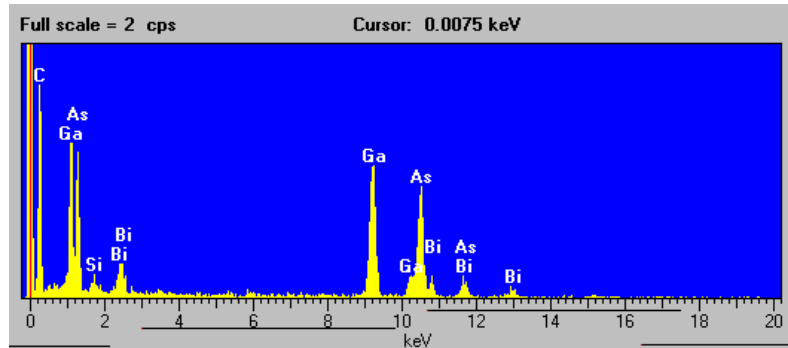
- atomic number dependence of X-ray yield (Z)*
- absorption in thicker specimens (A)**
- fluorescence of neighbouring lines (F)**

typical artefacts encountered in an EDX spectrum of a Si:Li detector:

- Si escape peaks 1.74keV below the true peak position*
- Si internal fluorescence peak at 1.74keV from detector deadlayer at surface contact*
- sum peaks if the count rates and the deadtime are too high*
- coherent Bremsstrahlung, depending on voltage and orientation*
- spurious X-rays from apertures (Mo, Pt, Ir) and pole-piece (Fe, Co)
- spurious X-rays from specimen mount (C mesh support, Cu grid)

The effects marked with an asterisk are automatically taken into account by the analysis software. For the absorption and fluorescence corrections (**) the specimen thickness must be known! Other effects have to evaluated manually.

example of X-ray spectrum from a 17nm thin GaAsBi layer



quantification procedures

Thus, for thin films, neglecting absorption and fluorescence, you can use the *k*-factor method by Cliff and Lorimer (cf. G. Cliff and G.W. Lorimer, J. Microsc. 103 (1975) 203-207) for relative quantification of concentrations, *c* from intensities, *I* if the concentration of one element is known:

$$c_1/c_2 = k_{1,2} I_1/I_2$$

Herein, the *k*-factor for one element is given by the product of ionisation cross-section and detector sensitivity, divided by the atomic weight. It is best to measure *k*-factors relative to a standard, using e.g. Si or Ti K-lines for various stoichiometric silicates and titanates, in order to avoid additional quantification errors!

For thicker specimens absorption and fluorescence need to be taken into account. Check: test if quantification of K- and L-lines gives consistent or at least similar results because in thicker samples the lower energetic L-lines can be strongly absorbed.



electron energy-loss spectroscopy (EELS)

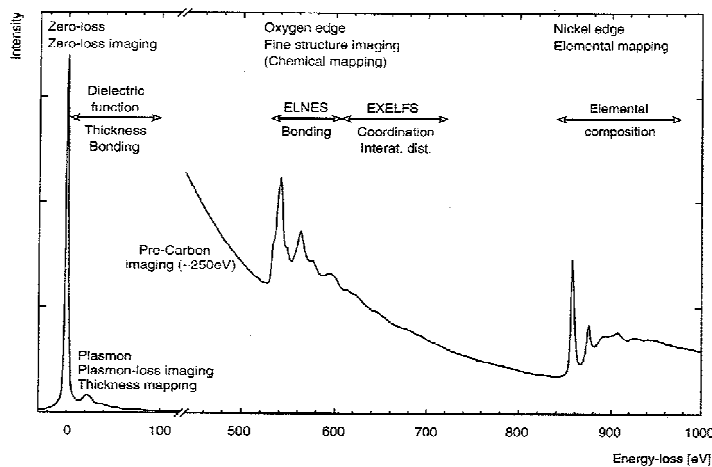
spectral information

- EELS analyses can be performed in a transmission electron microscope (TEM) with broad beam illumination or a scanning transmission electron microscope (STEM) with a focused electron beam.
- EELS measures the energy loss of electrons within the sample.
- An EELS spectrometer collects energy-loss spectra that can provide highly sensitive information about specimen thickness, elemental composition, valence, bonding and co-ordination.
- An imaging energy filter can in addition produce images or diffraction patterns of a narrow range of energy-losses.



electron energy-loss spectroscopy (EELS)

spectral information





electron energy-loss spectroscopy (EELS)

spectral information

rôle of specimen thickness:

- probability for n-fold inelastic scattering: Poisson statistics

$$P_n = (1/n!) (t/\lambda)^n \exp(-t/\lambda)$$

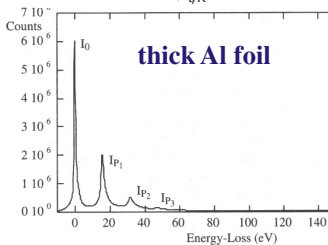
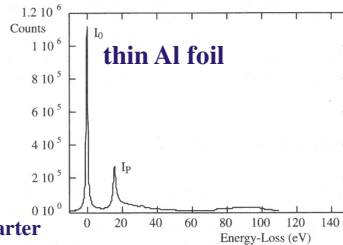
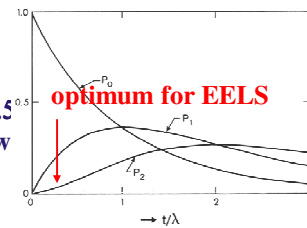
- relative thickness:

$$t/\lambda = \ln(I_{\text{ges}}/I_0) = \ln(1 + I_{\text{in}}/I_0)$$

systematic error: for larger thicknesses ($t/\lambda > 0.5$)

multiple inelastic scattering moves intensity away from the edge onset towards higher energies

--> deconvolution or multi-window approach



Williams & Carter

EEE 6395 Electron Microscopy of Semiconductor Structures

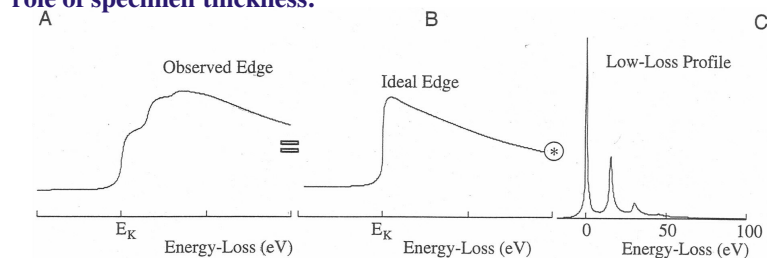
page 75



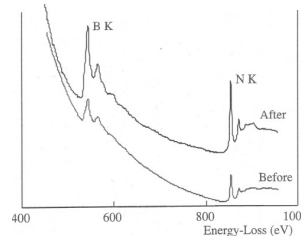
electron energy-loss spectroscopy (EELS)

spectral information

rôle of specimen thickness:



Deconvolution increases the jump ratio of the edges, improves the visibility of real details and eliminates false details (plasmon artefacts) due to multiple scattering.



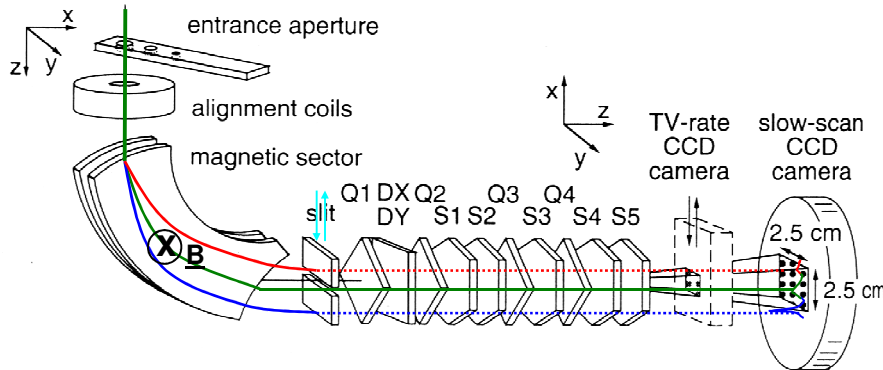
textbook by Williams & Carter

EEE 6395 Electron Microscopy of Semiconductor Structures

page 76

electron energy-loss spectroscopy (EELS)

spectrometers as energy analysers



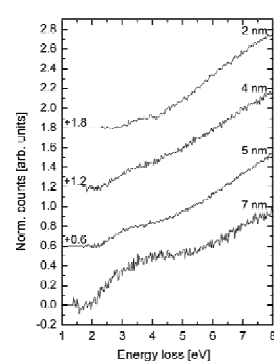
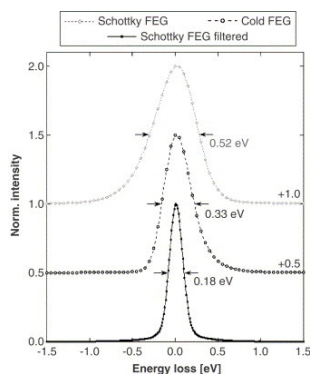
Gatan imaging filter (GIF) with 2D-detector (CCD or TV) to record EEL spectra (slit retracted) or energy-filtered images or diff. patterns (slit inserted)

electron energy-loss spectroscopy (EELS)

valence EELS

use low-loss EELS to

- get dielectric function from relationship $I \propto \Im m(-1/\epsilon)$ and Kramers-Kronig transformation
- directly determine the band-gap from fitting a function of form $(E - E_{\text{gap}})^{1/2}$ for direct band-gaps (cf. CdTe nanoparticles, right) and $(E - E_{\text{gap}})^{3/2}$ for indirect band-gaps

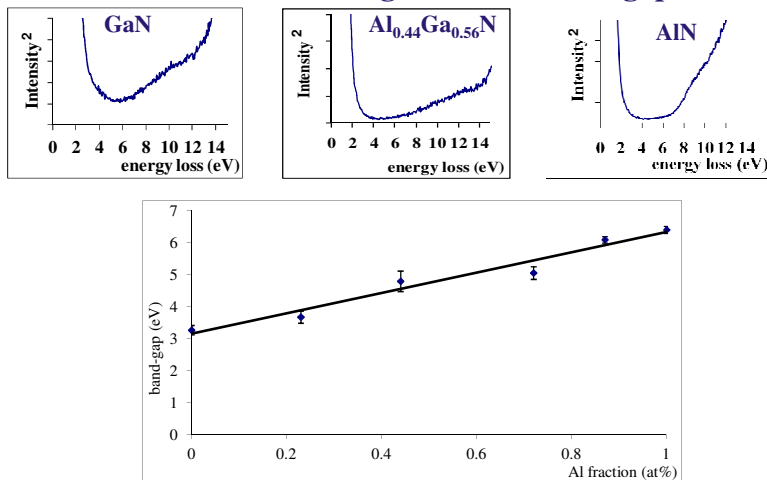


R. Erni and N.D. Browning, Ultramicroscopy **104** (2005) 176-192 & **107** (2007) 267-273



electron energy-loss spectroscopy (EELS)

valence EELS for measuring the direct band-gap



EELS from Al_xGa_{1-x}N: E_g (eV) = (3.14 - 0.20) + x (3.18 - 0.31)
H. Amari *et al.*, J. Phys. Conf. Ser. 326 (2011) 012039

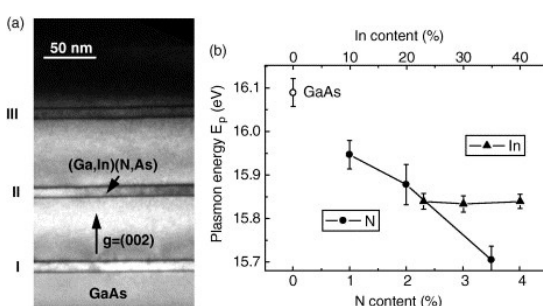


electron energy-loss spectroscopy (EELS)

chemical composition measurements

plasmon energy measurements

determine maximum position of plasmon loss and use tabulated values for many materials to get estimate of chemical composition!



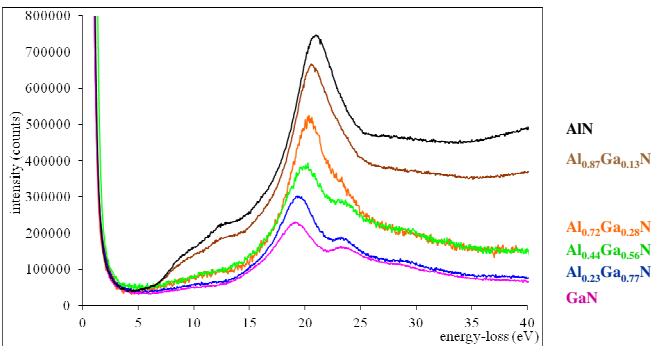
X. Kong, A. Trampert and K.H. Ploog, Micron 37 (2006) 465-472



electron energy-loss spectroscopy (EELS)

chemical composition measurements

plasmon energy measurements



plasmon energy shift in $\text{Al}_x\text{Ga}_{1-x}\text{N}$ is linear in composition:

$$E_p \text{ (eV)} = (19.12 - 0.16) + x(1.80 - 0.25)$$

H. Amari *et al.*, J. Phys. Conf. Ser. **326** (2011) 012039



electron energy-loss spectroscopy (EELS)

chemical composition measurements

inner shell (core loss) measurements

1. step: select thin region or deconvolute spectrum by low-loss
2. step: fit and subtract background
3. step: correct for exposure time
4. step: calculate scattering cross-section σ
5. step: choose between absolute vs. relative quantification

absolute: intensity of edge for N atoms:

$$I_N = N I_{\text{ges}} \sigma(U, \beta, \Delta E) / A$$

gives areal density N/A of atomic species

relative: concentration x of element A at constant thickness:

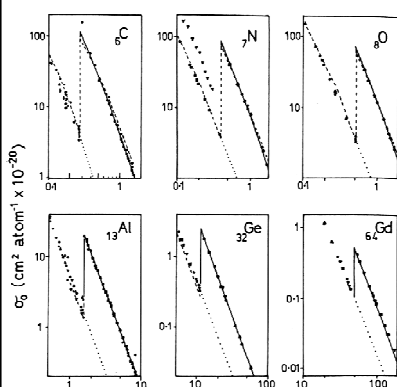
$$x_A = (I_A / \sigma_A) / \sum_i (I_i / \sigma_i)$$



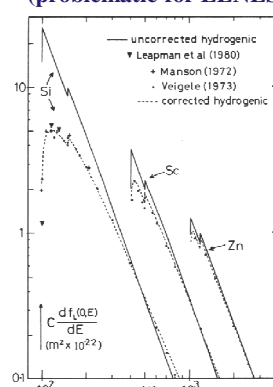
electron energy-loss spectroscopy (EELS)

calculation of scattering cross-sections

K-edges: fine



L-edges: usually OK
(problematic for ELNES)



M-edges: useless
(use experimental standards instead!)

comparison of theory (...hydrogenic modell, -- HS) with EELS / XAS from textbook by Egerton

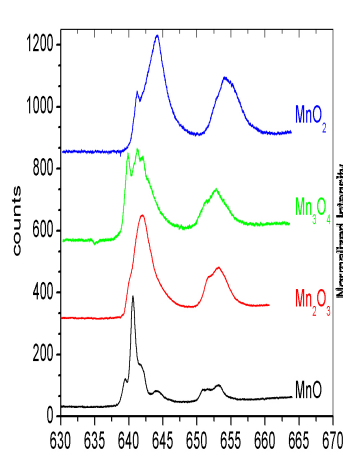
EEE 6395 Electron Microscopy of Semiconductor Structures

page 83

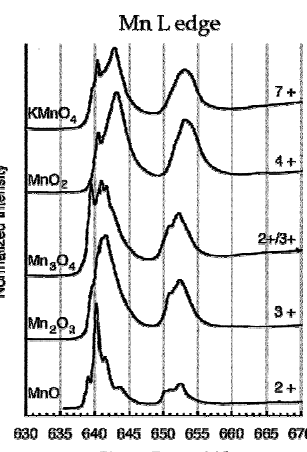


electron energy-loss spectroscopy (EELS)

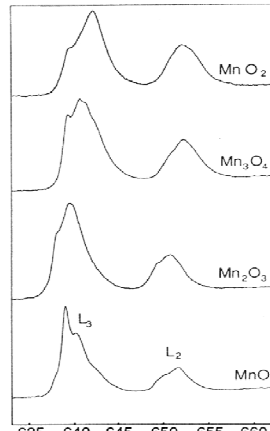
energy-loss near-edge structure (ELNES)



ELNES with Zeiss CRISP
Walther et al., Proc ICM-16
Sapporo, 2 (2006) 833



HR-XANES beam-line
Gilbert et al., J. Phys.
Chem. A 107 (2003) 2839



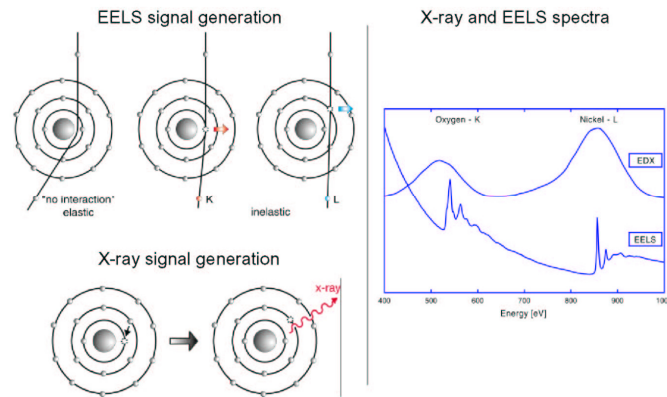
ELNES with VG STEM
Paterson & Krivanek,
Ultramic. 32 (1990) 319

EEE 6395 Electron Microscopy of Semiconductor Structures

page 84

comparison of EDXS with EELS

EELS and X-Ray Signal Generation



comparison of EDXS with EELS

EDXS

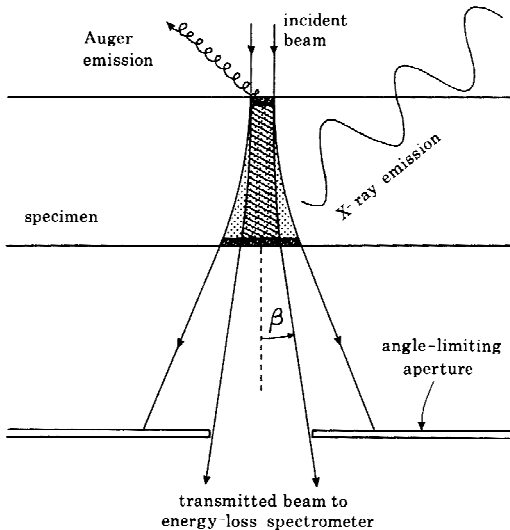
- X-rays provide elemental information only
- inefficient signal generation, collection and detection
- slow technique (minutes to hours for X-ray mapping)
- X-ray spectra can contain artefacts
- good detection efficiency for high Z elements
- energy resolution $>100\text{eV}$ causes frequent overlaps
- spectral processing standardised
- spatial resolution depends on specimen thickness ($>1\text{nm}$)

EELS

- elemental, chemical, and dielectric information
- very efficient in every respect – higher sensitivity for most elements
- fast technique (seconds to minutes for ETEM or spectrum imaging)
- EELS spectra usually have no such artefacts
- high detection efficiency for low Z elements
- energy resolution $\sim 1\text{eV}$ (0.15eV with monochromator) gives fewer overlaps
- more complex processing required
- spatial resolution depends on energy loss and collection aperture



comparison of EDXS with EELS



after: S.A. Collett, L.M. Brown and M.H. Jacobs, Proc. Conf. Quant. Microanalysis with High Spatial Resolution, Manchester, The Metals Society, London (1981) pp. 159-164



Textbooks for further reading

R.F. Egerton: Electron Energy-Loss Spectroscopy in the Electron Microscope, 2nd ed., Plenum, New York, (1996): the definitive EELS reference handbook for physicists, materials scientists and chemists

J.I. Goldstein, H. Yakowitz, D.E. Newbury, E. Lifshin, J.W. Colby, J.R. Coleman, R.B. Bolon and M.F. Ciccarelli: Practical Scanning Electron Microscopy: Electron and Ion Microprobe Analysis, Plenum, New York (1975): good overview over SEM

P.B. Hirsch, A. Howie, R.B. Nicholson, D.W. Pashley and M.J. Whelan: Electron Microscopy of Thin Crystals, Butterworths, London (1965): comprehensive treatment of diffraction contrast in TEM

D.C. Joy: Monte Carlo Modeling for Electron Microscopy and Microanalysis, Oxford University Press, New York and Oxford (1995): detailed models and program descriptions for BSE and EDXS analysis in SEM and STEM

R.J. Keyse, A.J. Garratt-Reed, P.J. Goodhew and G.W. Lorimer: Introduction to Scanning Transmission Electron Microscopy, Bios Scientific, Oxford (1998): brief introduction to STEM for engineers

L. Reimer: Transmission Electron Microscopy; Physics of Image Formation and Microanalysis, 2nd ed., Springer, Berlin (1989): a rather complicated but precise and reliable textbook for physicists

J.C. H. Spence: Experimental High-Resolution Electron Microscopy, 2nd ed., Oxford University Press, New York (1988): good handbook for HREM

D.B. Williams and C.B. Carter: Transmission Electron Microscopy, Springer, New York (1996): a very good general textbook (paperback in four volumes!)